

## Mode Mixing With Reduced Losses in Parabolic-Index Fibers

By D. MARCUSE

(Manuscript received January 13, 1976)

*We present design criteria for the construction of a modified parabolic-index fiber with intentional mode coupling. Mode coupling serves the purpose of reducing multimode pulse dispersion and is accomplished by introducing carefully designed index fluctuations into the fiber core or by controlled "random" bends of the fiber axis. Radiation losses due to mode coupling can be minimized by terminating the parabolic-index fiber core in an abrupt index discontinuity. The additional modes introduced by this step must be filtered out by periodic mode filters that consist of parabolic-index fiber sections without the refractive-index step.*

### I. INTRODUCTION

In multimode optical fibers, light pulses are carried by many modes. Such multimode operation limits the information-carrying capacity of an optical fiber communications system because of pulse spreading. At the fiber input, all modes receive part of the energy of the light pulse simultaneously. However, at the fiber output, the light pulse is stretched out in time because each mode (or mode group) travels at a different group velocity. The length of the stretched pulse is proportional to the fiber length. The amount of pulse spreading in a multimode fiber depends on its construction. The dependence of the group velocity of the modes on the mode labels is influenced by the distribution of the refractive-index profile of the fiber in radial direction.<sup>1</sup> Step-index fibers\* typically exhibit more pulse spreading than fibers with graded refractive-index distributions. Fibers whose index profiles show a parabolic (or square law) dependence on the radial coordinate have the property that all modes have nearly the same group velocity so that pulse spreading on parabolic-index fibers is nearly minimized.<sup>1</sup>

Our remarks so far apply to multimode transmission in perfect fibers where each mode propagates independently of all the other modes.

---

\* Step-index fibers have a core with constant refractive index and a lower index cladding.

Inhomogeneities of the axial distribution of the refractive index or geometrical imperfections of the fiber geometry tend to couple the modes among each other. Mode coupling has the undesirable consequence that some of the power is coupled to unguided radiation modes resulting in radiation losses.<sup>2</sup> On the other hand, coupling of the guided modes results in a continuous interchange of power between fast and slow modes so that a light pulse that is distributed over all the modes assumes a new shape. Instead of spreading according to the different group velocities of the independent modes, the light power carried by coupled modes is forced to travel at an average velocity and exhibits a narrower width, which spreads only proportionally to the square root of the fiber length.<sup>3</sup> Thus, mode coupling can be intentionally introduced to improve the pulse performance of multimode fibers.<sup>4</sup> However, this technique for improving the pulse performance must be used with great care to avoid an unacceptable increase in the power loss of the fiber.

To understand how mode coupling can be tailored to minimize losses, it is necessary to consider the coupling process in more detail. Each mode has a characteristic propagation constant  $\beta_M$ . The label  $M$  is used to identify the mode. A unique mode designation requires that  $M$  consists actually of two symbols representing the radial and azimuthal mode numbers. For simplicity, we combine the double label in the single symbol  $M$ . As mentioned before, mode coupling is provided by some deviation of the fiber from its perfect geometry and composition.<sup>5</sup> We use a function  $f(z)$  to describe the axial dependence of the deviation of the refractive-index distribution or of the core-radius deviation from their nominal, perfect values. In addition to this function of the length coordinate  $z$ , we need its Fourier transform which we define as

$$F(\theta) = \lim_{L \rightarrow \infty} \left\{ \frac{1}{\sqrt{L}} \int_0^L f(z) e^{i\theta z} dz \right\}. \quad (1)$$

Coupling between two modes labeled  $M$  and  $N$  is mediated by a particular Fourier component of  $f(z)$  according to the law<sup>2</sup>

$$\beta_M - \beta_N = \theta. \quad (2)$$

It is thus clear that two modes remain uncoupled if  $F(\theta) = 0$  for the particular  $\theta$  value required by (2). Furthermore, if the differences between the propagation constants of neighboring guided modes depend on the mode number,  $F(\theta) \neq 0$  is required over a certain range of  $\theta$  values if all guided modes are to be coupled. Using these rules and certain "selection rules," it has been demonstrated<sup>4</sup> that most guided modes of a step-index fiber can be coupled with very little radiation

loss if the Fourier spectrum (1) is limited to a carefully selected range, such that Fourier components exist for coupling the guided modes according to (2), but that coupling between guided and radiation modes [also obeying the law (2)] is prevented.

Mode coupling in parabolic-index fibers requires only a narrow spectrum of spatial frequencies  $\theta$  because the differences between propagation constants of neighboring modes are almost independent of the mode label. This feature of the modes of the parabolic-index fiber causes a problem since it makes it harder to discriminate between coupling among guided modes and coupling from guided to radiation modes. With an appropriate selection rule, coupling among guided modes of the step-index fiber has the property that the differences (2) increase with increasing mode number.<sup>4</sup> Cutting the Fourier spectrum (1) off at a maximum spatial frequency  $\theta = \theta_{\max}$  thus stops mode coupling at a given mode number, so that coupling between guided modes of lower order and modes with the highest mode numbers is prevented. Since only the highest-order modes are near (in mode number space) radiation modes, coupling between guided and radiation modes is thus avoided. Because of the almost constant differences between propagation constants of neighboring modes, this strategy fails in the parabolic-index fiber.

We show in this paper that we may couple the guided modes of a parabolic-index fiber and still avoid radiation losses by using a modified parabolic-index profile. An ideal parabolic-refractive-index profile has the form

$$n = n_0 \left[ 1 - \left( \frac{r}{a} \right)^2 \Delta \right] \quad |r| < \infty. \quad (3)$$

$r$  is the radial coordinate and  $\Delta/a^2$  determines the gradient of the index profile. The true parabolic-index profile cannot be realized because the refractive index of ordinary solid materials cannot be less than unity. Typical parabolic-index fibers have index profiles of the form

$$n = \begin{cases} n_0 \left[ 1 - \left( \frac{r}{a} \right)^2 \Delta \right] & |r| \leq a \\ n_2 = n_0(1 - \Delta) & a \leq |r| \leq b \\ 1 & b \leq |r| < \infty. \end{cases} \quad (4)$$

The cladding region  $a \leq |r| \leq b$  is usually so thick that, mathematically, we may assume  $b \rightarrow \infty$ . The guided modes do not carry significant amounts of power inside of the cladding region so that they behave almost as if they were guided by the ideal index distribution (3). Modes with significant amount of power in the cladding region are no longer guided but belong to the continuous spectrum of radia-

tion modes. By providing a narrow Fourier spectrum of spatial frequencies for the purpose of coupling the guided modes, we necessarily couple the highest-order guided modes to radiation and lose power.

The situation is changed if we modify the index profile to the following form:

$$n = \begin{cases} n_0 \left[ 1 - \left( \frac{r}{a} \right)^2 \Delta \right] & |r| \leq a \\ n_2 < n_0(1 - \Delta) & a < |r| \leq \infty \end{cases} \quad (5)$$

( $b = \infty$  was assumed for simplicity). The index profiles of (3), (4), and (5) are shown in Figs. 1a, 1b, and 1c. We divide the guided modes of the index profile (5), shown in Fig. 1c, into two classes. There are modes whose field distributions are essentially limited to the region  $0 \leq |r| \leq a$ . These modes have negligibly small field intensities in the region  $|r| \geq a$  and behave as though they belonged to the idealized medium defined by (3). Because modes of this kind are essentially the modes of the parabolic-index medium, we call them P-modes. There are, in addition, modes of order higher than the P-modes whose field distributions reach strongly into the region near  $r = a$ . These modes are guided by the index discontinuity at  $r = a$  and behave similar to the modes in a step-index fiber. For this reason we call them S-modes. The differences (2) between neighboring P-modes are nearly identical, while the differences between S-modes are much larger and, if an additional selection rule is introduced, increase with increasing mode number. If a narrow band of spatial Fourier components is provided to couple the P-modes among each other, S-modes will remain uncoupled from P-modes and also remain uncoupled among each other. Thus, we have achieved coupling among the P-modes and have improved their pulse performance. However, if S-modes were allowed to reach the detector, the pulse performance of the fiber would be degraded very seriously because of the different group velocities of P-modes and S-modes and the large group velocity spread among the S-modes. It is thus necessary to suppress S-modes before they reach the detector. This can be done easily by adding at the end of our fiber with index distribution (5) (or Fig. 1c) another fiber section that does not allow S-modes to propagate. A fiber with an index profile according to (3), or Fig. 1b, has this property.

The strategy just outlined would work if there were truly no coupling between P- and S-modes. Some residual coupling is, however, unavoidable because of imperfect fiber tolerances. A small amount of power will always be coupled from P-modes to S-modes causing a "noise" background to reach the detector. This unwanted noise can be reduced by installing mode filters periodically along the fiber. As mentioned above, mode filters for S-modes consist simply of fiber sections with an index profile according to (4), or Fig. 1b. If we construct a fiber whose

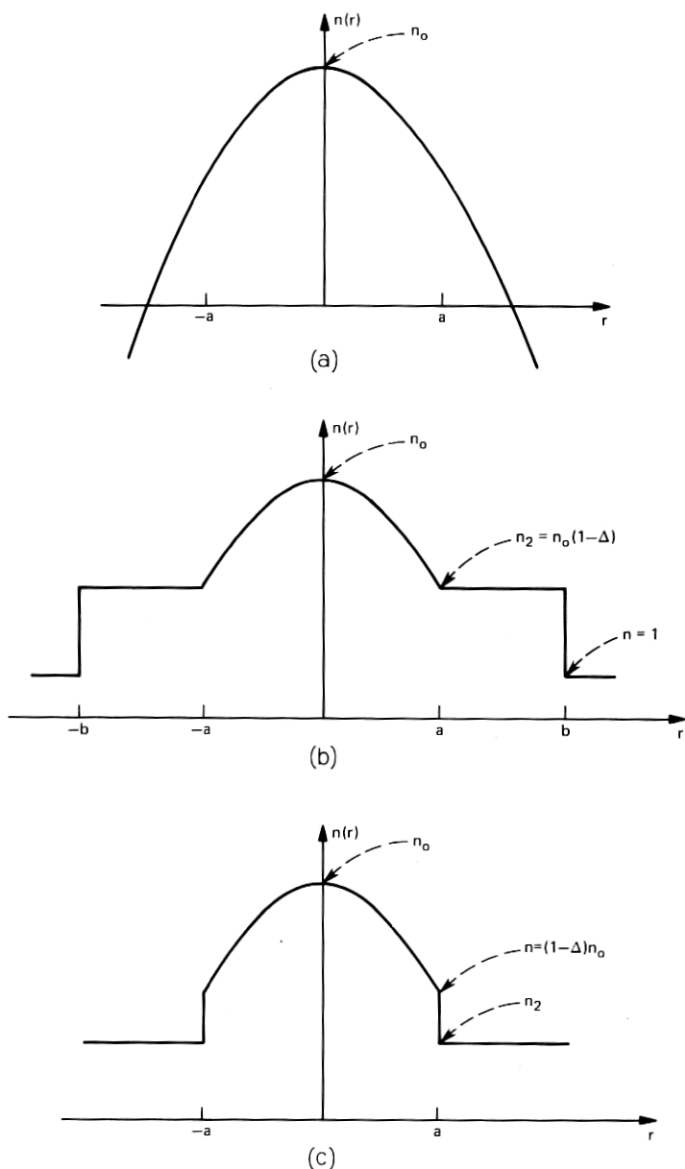


Fig. 1—(a) Ideal parabolic-index profile of eq. (3). (b) Truncated parabolic-index profile of eq. (4). This profile is used for mode filters. (c) Modified parabolic-index profile of eq. (5). This profile is used for the fiber with intentional mode coupling.

index profile is given by (5), or Fig. 1c, for most of its length, but which is changed to assume the form of (4) shown in Fig. 1b for relatively short sections periodically interspersed with the rest of the fiber, we obtain a fiber guide with mode filters for S-modes. Mode filters must

not be spaced too closely in order to avoid excessive losses. The additional loss occurs because we cannot avoid coupling between P-modes and a small group of S-modes that lie immediately adjacent (in mode number space) to P-modes. Along the boundary between P- and S-modes, mode spacing cannot be controlled so that we must assume that the intentionally introduced strong coupling mechanism will couple P-modes to their immediate S-mode neighbors along their common mode boundary. The mode filters strip away all S-modes, thus causing a small amount of loss of power that has been coupled to the S-mode group near the mode boundary. Design criteria for optimum mode filter spacings will be given in this paper.

If intentional mode coupling is achieved by introducing index fluctuations into the fiber core, the mode filters can be incorporated into the fiber by the same manufacturing process that was used to produce the intentional fiber "imperfections." On the mode filter sections, no strong coupling will be provided to avoid additional losses. We shall show later that coupling can also be provided by small bends of the fiber axis.

In the following chapters, we provide the necessary information to explain the mechanism and give design criteria for a modified parabolic-index fiber with mode coupling.

## II. MODE SPECTRUM OF THE MODIFIED PARABOLIC-INDEX FIBER

We have defined P-modes and S-modes in the introduction. P-modes have field distributions that have (negligibly) small values at the core boundary  $r = a$ . Their properties are nearly identical with the modes of the ideal, infinitely extended square-law medium. We may associate rays with these modes. The rays corresponding to P-modes spiral around the fiber axis in helical paths. Axial rays cross the fiber axis and move out to a turning point where the tangent to their path is parallel to the fiber axis. Spiraling rays encounter two turning points, one near the fiber axis and the other one at larger radii.<sup>1,6</sup> An approximate field description utilizes the fact that modes in weakly guiding fibers are nearly linearly polarized<sup>7</sup> (at least suitable superpositions of exact fiber modes are nearly linearly polarized). Their dominant transverse electric field component can be approximately expressed by the WKB approximation in the form<sup>1,6</sup>

$$E = A \frac{\cos\left(\psi - \frac{\pi}{4}\right) e^{-i\nu\phi} e^{-i\beta z}}{\left(\{[n(k)r]^2 - \beta^2\} r^2 - \nu^2\right)^{\frac{1}{2}}} \quad (6)$$

with

$$\psi = \int_{r_1}^r \frac{1}{r} \left(\{[n(r)k]^2 - \beta^2\} r^2 - \nu^2\right)^{\frac{1}{2}} dr. \quad (7)$$

$A$  is an amplitude coefficient, the integer  $\nu$  is the azimuthal mode number,  $\beta$  the propagation constant, and

$$k = \omega(\epsilon_0\mu_0)^{\frac{1}{2}}, \quad (8)$$

the propagation constant of plane waves in free space. The inner turning point  $r_1$  is the smaller root of the equation

$$\{[n(r)k]^2 - \beta^2\}r^2 - \nu^2 = 0. \quad (9)$$

Since the denominator of the expression in (6) vanishes, the WKB approximation seems to fail at the turning points. A more careful analysis (not used here) is capable of bridging the gap and extending the validity of the WKB solution across the turning points. The requirement of continuity of the field solutions across the turning points leads to the condition<sup>6,8</sup>

$$\int_{r_1}^{r_2} \frac{1}{r} (\{[n(r)k]^2 - \beta^2\}r^2 - \nu^2)^{\frac{1}{2}} dr = (2p + 1) \frac{\pi}{2}. \quad (10)$$

The upper turning point  $r_2$  is the larger root of eq. (9), the integer  $p$  is the radial-mode number. Equation (10) defines the propagation constant  $\beta$  and is called the eigenvalue equation. For P-modes we have  $r_2 < a$  and obtain by substitution of (5) or (3) into (10) the expression

$$\beta = \left\{ n_0^2 k^2 - 2n_0 \frac{k}{a} (2\Delta)^{\frac{1}{2}} (2p + \nu + 1) \right\}^{\frac{1}{2}}. \quad (11)$$

S-modes reach the core boundary. It is well known that an abrupt index change at the core boundary forces the electric field intensity to assume very low values at  $r = a$ . For all modes, with the exception of modes very close to cutoff, it is permissible to approximate the actual value of the electric field by  $E = 0$  at  $r = a$ . This condition in conjunction with (6) and (7) leads to the following eigenvalue equation for S-modes,

$$\int_{r_1}^a \frac{1}{r} (\{[n(r)k]^2 - \beta^2\}r^2 - \nu^2)^{\frac{1}{2}} dr = (2p + \frac{3}{2}) \frac{\pi}{2}. \quad (12)$$

Substitution of (5) and integration leads to

$$\begin{aligned} & [(\kappa_0 a)^2 - 2(n_0 k a)^2 \Delta - \nu^2]^{\frac{1}{2}} \\ & - \nu \left[ \arctan \left( \frac{\frac{1}{2}(\kappa_0 a)^2 - \nu^2}{\nu [(\kappa_0 a)^2 - 2(n_0 k a)^2 \Delta - \nu^2]^{\frac{1}{2}}} \right) + \frac{\pi}{2} \right] \\ & + \frac{(\kappa_0 a)^2}{2n_0 k a (2\Delta)^{\frac{1}{2}}} \left[ \arcsin \left( \frac{(2n_0 k a)^2 \Delta - (\kappa_0 a)^2}{[(\kappa_0 a)^4 - (2n_0 k a \nu)^2 2\Delta]^{\frac{1}{2}}} \right) + \frac{\pi}{2} \right] \\ & = (2p + \frac{3}{2})\pi \quad (13) \end{aligned}$$

with

$$\kappa_0^2 = n_0^2 k^2 - \beta^2. \quad (14)$$

The guided and radiation modes of the modified parabolic-index fiber can be displayed in mode-number space. Each mode is characterized by two integers, the azimuthal mode number  $\nu$  and the radial mode number  $p$ . Mode-number space displays the values of  $\nu$  and  $p$  in the plane shown in Fig. 2. For P-modes we can introduce a compound mode number

$$M = 2p + \nu + 1 \quad (15)$$

and express the propagation constant (11) in the form,

$$\beta = \left\{ (n_0 k)^2 - 2 \frac{n_0 k}{a} (2\Delta)^{1/2} M \right\}^{1/2}. \quad (16)$$

Modes with constant values of  $M$  have the same propagation constants and lie on diagonal dotted lines, two of which are shown in Fig. 2. Cutoff for the S-modes is defined by the condition

$$\beta = n_2 k \quad (17)$$

or

$$\kappa_0 = (n_0^2 - n_2^2)^{1/2} k. \quad (18)$$

When we substitute (18) into (13), we obtain an implicit equation for the mode boundary between S-modes and radiation modes shown in Fig. 2 as the solid line. The boundary between P-modes and S-modes is defined by the condition in (16) written in the form

$$(\kappa_0 a)^2 = 2n_0 k a (2\Delta)^{1/2} M \quad (19)$$

and from

$$(\kappa_0 a)^2 = 2(n_0 k a)^2 \Delta + \nu^2. \quad (20)$$

Equation (20) expresses the requirement that the transition from P-modes to S-modes occurs when the turning point falls on the core boundary and is obtained by combining (5), (9), (14), and the condition  $r = r_2 = a$ . By eliminating  $\kappa_0 a$  from (19) and (20), we obtain a functional relation between  $\nu$  and  $p$  which was used to calculate the dash dotted mode boundary shown in Fig. 2. This figure was computed with the help of the following parameters,

$$\left. \begin{aligned} n_0 &= 1.53 \\ n_2 &= 1.5 \\ ka &= 150 \\ \Delta &= 0.0098 \end{aligned} \right\}. \quad (21)$$

These values lead to the following value for the refractive index at the core boundary:  $n_0(1 - \Delta) = 1.515$ .



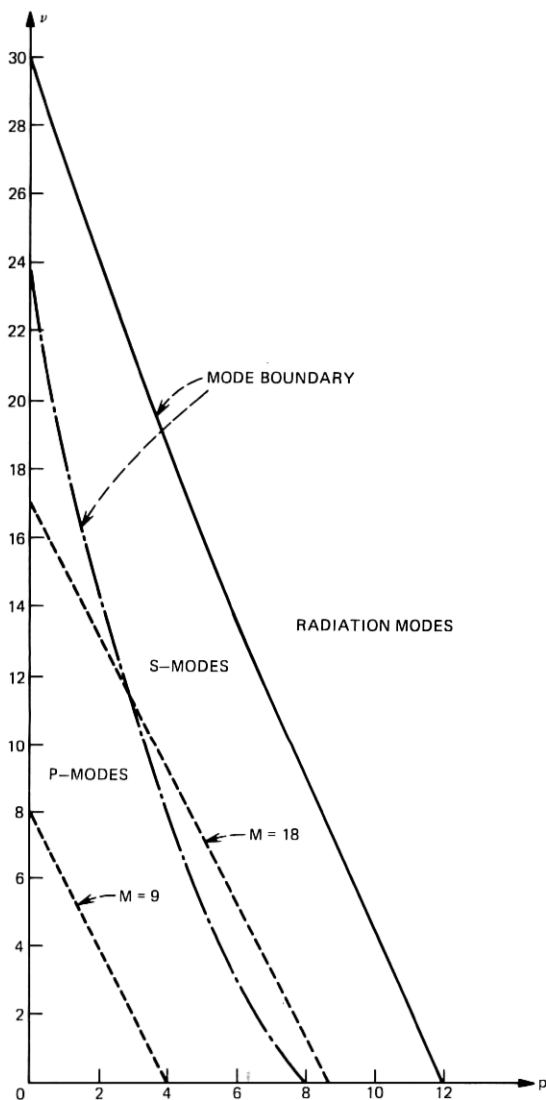


Fig. 2—Mode number space. The solid line is the boundary between S-modes and radiation modes. The dash-dotted line is the boundary between S-modes and P-modes. The dotted lines labeled  $M = 9$  and  $M = 18$  are curves of constant compound mode number  $M$ .  $M = 18$  is used as approximate mode boundary.

For the purpose of designing a coupling mechanism for the P-modes, we need to know the differences between the propagation constants of the modes. If we let  $\nu$  change by  $\delta\nu$  and  $p$  by  $\delta p$ , we compute from

the eigenvalue equation for the P-modes in the form (19),

$$\frac{\delta\kappa_0}{\kappa_0} = \frac{\delta M}{2M} \quad (22)$$

with

$$\delta M = 2\delta p + \delta\nu. \quad (23)$$

For the S-modes, we find from (13)

$$\frac{\delta\kappa_0}{\kappa_0} = \frac{\pi(\delta p) + \frac{1}{2}(\delta\nu) \left[ \arctan\left(\frac{\frac{1}{2}(\kappa_0 a)^2 - \nu^2}{\nu S}\right) + \frac{\pi}{2} \right]}{(2p + \frac{3}{2})\pi + \nu \left[ \arctan\left(\frac{\frac{1}{2}(\kappa_0 a)^2 - \nu^2}{\nu S}\right) + \frac{\pi}{2} \right] - S} \quad (24)$$

with the abbreviation

$$S = [(\kappa_0 a)^2 - 2(n_0 k a)^2 \Delta - \nu^2]^{\frac{1}{2}}. \quad (25)$$

The difference of the propagation constants follows from (14):

$$\delta\beta = -\frac{\kappa_0^2}{\beta} \frac{\delta\kappa_0}{\kappa_0}. \quad (26)$$

We have plotted values for  $|\delta\beta a|$  in Fig. 3. These values were computed from (22) and (26) for P-modes and from (13), (24), and (26) for S-modes using the numbers in (21). We also assumed that  $\delta M = \pm 1$ . For P-modes,  $\delta M = \pm 1$  clearly yields the least separation between guided modes. ( $\delta M = 0$  would lead to  $\delta\beta = 0$  and is excluded.) Just as in the case of the step-index fiber, we introduce a selection rule by properly designing the coupling mechanism (see Section III below). The selection rule is

$$\delta\nu = \pm 1. \quad (27)$$

We may now achieve a transition between neighboring modes with  $|\delta M| = 1$  in two different ways. We can either use

$$\delta\nu = \pm 1, \quad \delta p = 0 \quad (28)$$

or

$$\delta\nu = \pm 1, \quad \delta p = \mp 1, \quad (29)$$

where the upper or lower set of signs belong together respectively. All other combinations lead to bigger values of  $|\delta M|$  and larger differences for the separation between the S-modes.

Figure 3 shows that the values of  $|\delta\beta a|$  for P-modes are very nearly independent of the mode number  $M$ . By using a Fourier spectrum (1) with spatial frequencies in the range  $\theta a = 0.14$  to  $0.1415$ , we couple all neighboring P-modes with  $|\delta M| = \pm 1$ . The hatched area in Fig. 3 labeled "S-modes" indicates the range of  $|\delta\beta a|$  values that occurs for

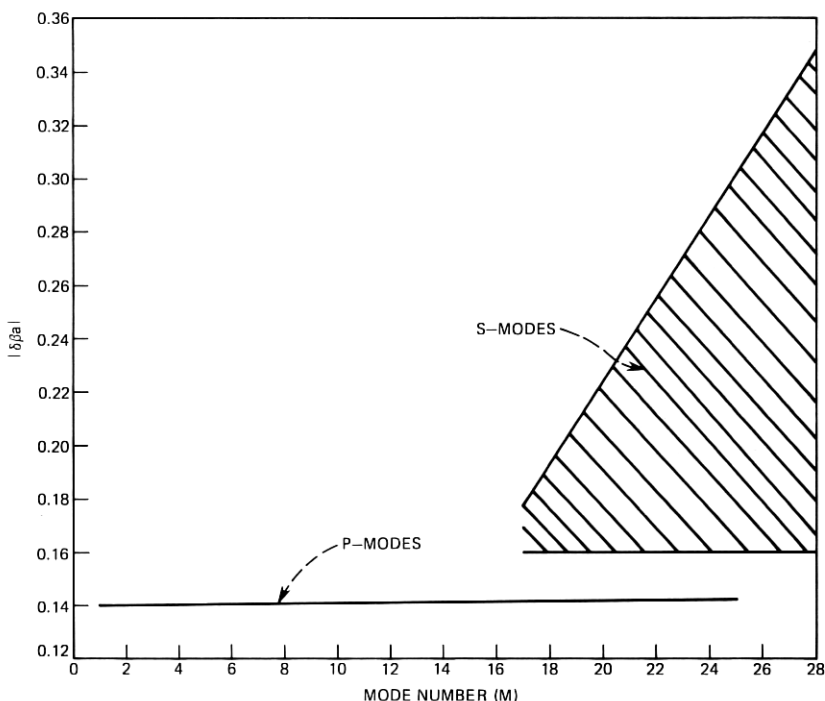


Fig. 3—The differences of propagation constants of adjacent modes with  $|\delta M| = 1$  as functions of the compound mode number  $M$ .

a given value of  $M$ . It is apparent how widely the differences between S-modes with  $|\delta M| = \pm 1$  vary. Typically, the combination (28) leads to smaller  $\delta\beta$  differences. However, even the smallest spacing between adjacent S-modes is so much larger than the corresponding spacing between P-modes that it should be relatively easy to design the coupling mechanism so that S-modes are not intentionally coupled among each other. The differences between adjacent P-modes and S-modes along the dash-dotted mode boundary in Fig. 2 cannot be calculated from our simplified theory, so that we must assume that P-modes, lying along the mode boundary, may be coupled to their S-mode neighbors.

We have now proved that P-modes can be coupled among each other by a spatial Fourier spectrum of very narrow width and that it is relatively easy to discriminate between P-mode and S-mode coupling. It remains to discuss mode coupling, study the degradation of pulse performance that results from coupling a few S-modes along the mode boundary to P-modes, and to discuss the performance of the mode filters.

### III. MODE COUPLING AND PULSE SPREADING

Mode coupling is provided by implanting a refractive-index perturbation into the fiber core.<sup>2</sup> Instead of the index distribution  $n$  given in (5), we now use a perturbed refractive-index distribution  $\mathbf{n}$  so that we have

$$\mathbf{n}^2 - n^2 = \frac{r}{a} f(z) \cos \phi \quad |r| \leq a. \quad (30)$$

The dependence of (30) on  $\cos \phi$  imposes the selection rule (27).<sup>2</sup> Without such a selection rule we could not uncouple P-modes and S-modes. The linear  $r$  dependence indicated in (30) is quite arbitrary. It is necessary that (30) vanishes at  $r = 0$  in order to have a well defined value of the function at this point. The linear  $r$  dependence is not only the simplest function that vanishes at  $r = 0$  but also one for which the coupling coefficient can be evaluated. Other  $r$  dependent functions could be used as factors in (30). The function  $f(z)$  is assumed to be a random function with the narrow Fourier spectrum (1) that assures coupling among the P-modes but prevents coupling between P-modes and S-modes.

The system of coupled P-modes can be described by coupled-power equations.<sup>2</sup> The coupling coefficients are obtained by solving overlap integrals including the function (30) multiplied with the electric field functions of the two modes whose coupling is to be evaluated. The P-modes are described very well by the Laguerre-Gaussian field solutions of the ideal parabolic-index distribution (3).<sup>9,10,11</sup> We obtain for the power-coupling coefficients<sup>2</sup>:

$$h_{\nu p, \nu-1, p} = K(p + \nu) \quad (31)$$

$$h_{\nu p, \nu-1, p+1} = K(p + 1) \quad (32)$$

$$h_{\nu p, \nu+1, p} = K(p + \nu + 1) \quad (33)$$

$$h_{\nu p, \nu+1, p-1} = Kp \quad (34)$$

with

$$K = \frac{k}{16n_0^3 a (2\Delta)^{\frac{1}{2}}} \langle F^2(\theta) \rangle. \quad (35)$$

The symbol  $\langle \rangle$  indicates that an ensemble average has been taken. The argument of the Fourier spectrum function (1) is the appropriate difference of the propagation constants of the coupled modes according to (2). [See eq. (75).]

It is our intention to solve the coupled-power equations for the P-modes with the coupling coefficients given by (31) through (35). The coupling mechanism postulated by the refractive-index perturbation (30) couples a given mode  $(\nu, p)$  to its neighbors  $(\nu + 1, p)$ ,

$(\nu - 1, p + 1)$ ,  $(\nu - 1, p)$ , and  $(\nu + 1, p - 1)$ . In the first two cases, the  $M$  number is increased by one while it is decreased by one in the third and fourth case. The coupled-power equations thus assume the form<sup>2</sup>

$$\begin{aligned} \frac{\partial P_{\nu,p}}{\partial z} + \frac{1}{v_M} \frac{\partial P_{\nu p}}{\partial t} + \alpha P_{\nu p} = & h_{\nu p, \nu+1, p} (P_{\nu+1, p} - P_{\nu p}) \\ & + h_{\nu p, \nu-1, p+1} (P_{\nu-1, p+1} - P_{\nu p}) + h_{\nu p, \nu-1, p} (P_{\nu-1, p} - P_{\nu p}) \\ & + h_{\nu p, \nu+1, p-1} (P_{\nu+1, p-1} - P_{\nu p}). \end{aligned} \quad (36)$$

We have indicated by our notation that the group velocity  $v_M$  depends only on the compound mode number  $M$  defined by (15) and not on the individual values of  $\nu$  and  $p$ . In addition, all modes are assumed to suffer the same loss  $\alpha$  caused by absorption and random scattering processes.

To be able to solve equation system (36), we assume that modes with equal values of the compound mode number  $M$  carry equal amounts of power. It is not obvious that this must be the case, but we may argue that modes with equal mode number  $M$  have identical propagation constants and, thus, are coupled among each other by the zero-spatial-frequency component of  $F(\theta)$ . The zero-frequency components of random distortions tend to be very large. Consider, for example, the departures from perfect straightness of the fiber axis. No fiber in actual use is ever perfectly straight. In fact, its slow variations tend to be particularly large so that its power spectrum peaks at zero spatial frequencies. This fact has been observed whenever power spectra of fiber distortions have been measured.<sup>12,13</sup> Consequently, we assume that modes with equal values of  $M$  are strongly coupled and, hence, equally populated by a coupling process that is not explicitly taken into account. It is only incorporated into the analysis by assuming that modes with the same values of  $M$  carry equal amounts of power. Making this assumption and substituting (31) through (35) into (36) allows us to write,

$$\left. \begin{aligned} P_{\nu p} &= P_M \\ P_{\nu+1, p} &= P_{\nu-1, p+1} = P_{M+1} \\ P_{\nu-1, p} &= P_{\nu+1, p-1} = P_{M-1} \end{aligned} \right\} \quad (37)$$

and

$$\begin{aligned} \frac{\partial P_M}{\partial z} + \frac{1}{v_M} \frac{\partial P_M}{\partial t} + \alpha P_M = & K[(M + 1)(P_{M+1} - P_M) \\ & - M(P_M - P_{M-1})]. \end{aligned} \quad (38)$$

If the number of guided modes is very large, we may regard them as a quasi-continuum and treat  $M$  approximately as a continuous vari-

able.<sup>14</sup> This assumption allows us to write the equation system (38) as a partial differential equation,<sup>2</sup>

$$\frac{\partial P_M}{\partial z} + \frac{1}{v_M} \frac{\partial P_M}{\partial t} = -\alpha P_M + K \frac{\partial}{\partial M} \left[ M \frac{\partial P_M}{\partial M} \right]. \quad (39)$$

Using (16), we can approximate the inverse group velocity in the following way

$$\frac{1}{v_M} = \frac{1}{c} \frac{\partial \beta}{\partial k} = \frac{n_0}{c} + WM^2 \quad (40)$$

with the abbreviation

$$W = \frac{\Delta}{n_0 c (ka)^2}. \quad (41)$$

$c$  is the velocity of light in vacuum. We have indicated in Section I that a group of S-modes along the mode boundary between P- and S-modes are coupled to the P-modes. These modes have different group velocities. We incorporate this mode group into our theory by assuming that the modes with the highest value of  $M$ ,  $M = N$ , have a group velocity that differs from the law given by (40) for P-modes. Thus, we use

$$\frac{1}{v_M} = \frac{n_0}{c} + W[M^2 + \rho N^2 \delta(M - N)]. \quad (42)$$

The parameter  $\rho$  is the relative amount by which the inverse velocity difference  $1/v_M - n_0/c$  of the mode group with  $M = N$  differs from the normal value. If the S-modes followed the law for the P-mode group velocity, we would have for the mode group with  $M = N$

$$\frac{1}{v_N} = \frac{n_0}{c} + WN^2. \quad (43)$$

Equation (42) states instead that the highest-mode group has inverse group velocity

$$\frac{1}{v_N} = \frac{n_0}{c} + (1 + \rho)WN^2. \quad (44)$$

We solve the time-dependent coupled-power equations in the usual way.<sup>2</sup> First, the time-independent problem is solved. The only difference from the normal procedure is that, in our present case, we do not assume that the highest-mode group is depleted by a loss process. Thus, instead of requiring  $P_N = 0$ , we assume that power outflow stops at  $M = N$  and require correspondingly

$$\frac{\partial P_M}{\partial M} = 0 \quad \text{at} \quad M = N. \quad (45)$$

The time-independent problem, thus, has the solution

$$P_M = e^{-\alpha z} \sum_{i=0}^{\infty} c_i \frac{J_0(u_i \sqrt{M/N})}{\sqrt{N} J_0(u_i)} e^{-\sigma_i z}. \quad (46)$$

The parameters  $u_i$  are the roots of the Bessel function  $J_1(x) = 0$  with  $u_0$  defined as zero; thus,

$$u_i = 0, 3.832, 7.016, 10.123, \dots \quad (47)$$

The eigenvalues are

$$\sigma_i = K \frac{u_i^2}{N} \quad (48)$$

with  $K$  of (35). The coefficients  $c_i$  determine the initial power distribution at  $z = 0$ . For large values of  $z$ ,  $P_m$  reaches its steady-state solution

$$P_M = \frac{c_0}{\sqrt{N}} e^{-\alpha z}, \quad (49)$$

which indicates that all modes carry equal amounts of power.

The time-dependent, steady-state solution is known to represent a pulse with gaussian shape.<sup>2,3</sup> Its full width (in time) between  $1/e$  points is given by second-order perturbation theory<sup>2</sup> and can be calculated to assume the following form:

$$T = T_0 \left( 1 + \frac{5\rho}{N} \right). \quad (50)$$

For  $\rho = 0$ , we obtain the pulse width of P-modes that are completely independent of the S-modes,

$$T_0 = \sqrt{L} \frac{2^{1/4} n_0^{1/2} \Delta^{5/4} N^{5/2}}{kc(ka)^{3/2} [\langle F^2(\theta) \rangle]^{1/2}}. \quad (51)$$

$L$  is the length of the fiber that has been traversed by the pulse. The pulse width spreads only proportional to the square root of the distance traveled. Equation (50) shows that the group of S-modes that is coupled to the P-modes widens the pulse more if its group velocity departs more from that of the P-modes—that is, with increasing values of  $\rho$ . Its influence is reduced with increasing values of the maximum mode number  $N$ .

A comment needs to be made regarding our analysis. We have calculated the impulse-response width (50) by treating the mode boundary between P- and S-modes as being parallel to the lines  $M = \text{const}$ . Figure 2 shows that this is not strictly true. In addition, it is not true that all S-modes along the mode boundary have equal group velocities. Our result must thus be regarded as an estimate and

we must use an average group velocity for the S-modes. For  $M = N$ , we use the value that is obtained by setting  $\nu = N/1.5$  in (19) and (20) and obtain,

$$N = [0.573n_0ka\sqrt{2\Delta}]_{\text{int}}. \quad (52)$$

The subscript "int" attached to the bracket indicates that the nearest integer to the number in brackets must be taken. The approximate mode boundary (52) is shown in Fig. 2 as the dotted line labeled  $M = 18$ .

#### IV. THE INFLUENCE OF RESIDUAL COUPLING BETWEEN P- AND S-MODES

If the intentionally introduced coupling were the only mechanism by which the guided modes interact, we would have no further problem. However, residual coupling between all the modes is unavoidable so that we must consider the problem of power coupling from P-modes to S-modes and vice versa.

If the P-modes carry light pulses, some of their power will couple to S-modes. Since S-modes travel with different group velocities, the power they receive from P-modes spreads out and forms an almost continuous background of noise power. Some of this power is coupled back into P-modes so that this noise background reaches the detector even if we filter out the S-modes before they reach the fiber end. Periodically spaced mode filters will reduce this noise problem, but filters increase the overall losses of the system so that it is necessary to reach a compromise between excess loss due to mode filters and undesirable noise caused by unintentional S-mode coupling.

We treat the noise problem in two stages. First, we consider the power-coupling process from P-modes to S-modes, and in the next step we allow this power to couple back to the P-modes.

Consider the equation system<sup>2</sup>

$$\frac{\partial Q_n}{\partial z} + \frac{1}{w_n} \frac{\partial Q_n}{\partial t} = \sum_{\mu} H_{n\mu} P_{\mu}. \quad (53)$$

These equations describe only coupling from P-modes to S-modes. Coupling in the reverse direction is ignored as are losses. For weak coupling in short, low-loss fiber sections, this equation system is a reasonable approximation to the complete coupled power equation.  $H_{n\mu}$  represents the residual, undesired coupling mechanism; the summation extends over all P-modes and the indexing system is simplified by using one symbol for the complete set of mode labels. By using a double Fourier integral transformation, it is possible to derive the following solution of (53),

$$Q_n = \frac{1}{2} \left( \sum_{\mu} H_{n\mu} E_{\mu} \right) \frac{w_n v}{v - w_n} \left[ \operatorname{erf} \left( \frac{t - z/v}{T/2} \right) - \operatorname{erf} \left( \frac{t - z/w_n}{T/2} \right) \right], \quad (54)$$



which is based on the assumptions that the pulses carried by the P-modes travel with a uniform velocity  $v$  (these pulses are strongly coupled by the intentional coupling mechanism) and that their shape is gaussian,<sup>2,3</sup>

$$P_{\mu} = A_{\mu} \exp \left[ - \frac{(t - z/v)^2}{(T/2)^2} \right] \quad (55)$$

with energy content

$$E_{\mu} = \int_{-\infty}^{\infty} P_{\mu} dt, \quad (56)$$

and that the S-modes are slower than the P-modes,

$$w_n < v \quad \text{for all } n. \quad (57)$$

The shape of the pulse carried by one S-mode is shown in Fig. 4 as the solid line. The shape of the P-mode pulses is indicated by the dotted line; the relative height of the two pulses is of no significance. The width of the S-pulse is

$$\delta z = t(v - w_n) = (v - w_n) \frac{z}{w_n}. \quad (58)$$

Because the P-pulses are spaced as closely as possible to maximize the information rate, we may safely assume that the S-pulses overlap after a distance  $z$  that is short compared to the total length of the fiber. The number of S-pulses that overlap at any given point is, on average,

$$M_s = \frac{\delta z}{D} = \frac{v - w_n}{w_n} \frac{z}{D}, \quad (59)$$

where  $D$  indicates the spatial separation between the original P-pulses.

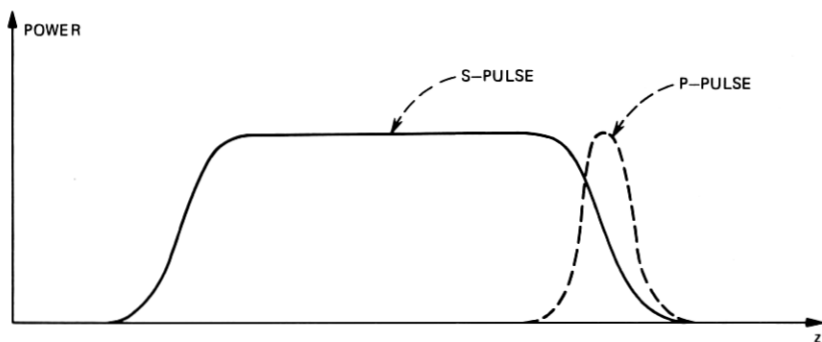


Fig. 4—The solid line is the shape of the S-pulse that results from coupling of P-mode power whose shape is indicated by the dotted line. The relative height of the two pulses is of no significance.

The average power carried by a given S-mode is, thus,

$$Q_n = M_s Q_n = v \frac{z}{D} \sum_{\mu} H_{n\mu} E_{\mu}. \quad (60)$$

[The difference of the two error functions in the bracket in (54) assumes the value 2 over most of the region where its value does not vanish. Equation (60) can also be obtained directly from (53).]

We have now determined the average power in a given S-mode due to unintentional power coupling from the P-modes. We have also convinced ourselves that the S-modes do not carry pulses, because of extensive pulse overlap, but carry a quasi-continuous background noise signal.

The amount of noise power that is coupled back from S-modes into P-modes is obtained from the time-independent coupled-power equations<sup>2</sup>

$$\frac{\partial \bar{P}_v}{\partial z} = \sum_n H_{vn} Q_n. \quad (61)$$

This equation is solved by simple integration. Summing over all modes and substituting (60) yields the following expression for the total noise power that is carried by all the P-modes,

$$N_p = \sum_v \bar{P}_v = v \frac{z^2}{2D} \sum_v \sum_n \sum_{\mu} H_{vn} H_{n\mu} E_{\mu}. \quad (62)$$

Greek summation symbols are used to indicate summation over P-modes while Latin symbols express summation over S-modes.

We assume that the fiber length between mode filters is  $z = d$ . At the end of the fiber of length  $L$ , we collect the noise contribution from  $L/d$  fiber sections between mode filters. The total noise is, thus,

$$N_t = \frac{vLd}{2D} \sum_v \sum_{\mu} \sum_n H_{vn} H_{n\mu} E_{\mu}. \quad (63)$$

So far we have ignored absorption and scattering losses. If all modes suffer identical losses, we only need to multiply (63) by the total loss that a signal suffers in traveling through the fiber. However, since our objective is to derive an expression for the signal-to-noise ratio, the absorption loss drops out in the end because signal and noise suffer identical losses. The average signal power at the end of the fiber is

$$S = \frac{1}{T} \sum_{\mu} E_{\mu}. \quad (64)$$

The signal-to-noise ratio at the fiber end is, therefore,

$$\frac{S}{N_t} = \frac{2D}{vTLd} \frac{\sum_{\mu} E_{\mu}}{\sum_{v,\mu} \sum_n H_{vn} H_{n\mu} E_{\mu}}. \quad (65)$$

If the unintentional coupling coefficients  $H_{nm}$  were known, we could calculate the signal-to-noise ratio from (65). Equation (65) tells us that the signal-to-noise ratio improves as the spacing  $D$  between pulses is increased or the pulse width  $T$  is decreased. The signal-to-noise ratio deteriorates with increasing unintentional coupling strength, in fact this decrease is inversely proportional to the square of the coupling strength. The signal-to-noise ratio decreases linearly with total fiber length  $L$  and with increasing fiber length  $d$  between mode filters. It is thus advantageous to space the mode filters as closely as the additional loss that filters introduce will allow.

For practical purposes, it will be necessary to obtain information about the unintentional mode coupling by making signal-to-noise measurements on a representative fiber sample. The signal-to-noise ratio of a fiber sample of length  $L_c$  follows from (65) if we set  $L = d = L_c$ . We may use pulses of length  $T_c$  for this measurement ( $T_c$  or  $T$  are measured at the end of each fiber) and use a pulse spacing  $D_c$  for the calibration measurement. This allows us to express the signal-to-noise ratio of a fiber with mode filters in terms of the measured signal-to-noise ratio  $(s/n)_c$  of a representative fiber sample,

$$\frac{S}{N_t} = \frac{DT_c L_c^2}{D_c T L d} (s/n)_c. \quad (66)$$

## V. LOSSES CAUSED BY MODE FILTERS

We explained in the introduction that mode filters are required to suppress the buildup of power in the S-modes. A mode filter is simply a section of fiber—without the mechanism for intentional mode coupling for P-modes—whose refractive index profile is modified from the shape of Fig. 1c (used for most of the fiber) to the shape of Fig. 1b.

Mode filters introduce additional losses because the strong coupling mechanism provided for the P-modes couples these modes to a group of S-modes immediately adjacent to the common mode boundary. Let us first consider how many modes there are for a given compound mode number. If we count the number of combinations of  $\nu$  and  $p$  that lead to a fixed value of  $M$  defined by (15), we find the following expression,

$$N_M = \left[ \frac{M-1}{2} \right]_{\text{int}} + 1. \quad (67)$$

The subscript "int" indicates in this case that the integer smaller than the number in brackets must be taken. For simplicity we use the approximation

$$N_M \approx \frac{M}{2}. \quad (68)$$

As a further approximation, we replace the mode boundary by the straight line labeled  $M = 18$  in Fig. 2. The total number of P-modes is now approximately

$$N_{T_p} = \sum_{M=1}^N \frac{M}{2} = \frac{1}{4}N(N+1). \quad (69)$$

Because of the strong intentional coupling, each P-mode and each mode in a group of  $N_N$  S-modes along the common mode boundary carries the same amount of energy. The energy reaching the  $\sigma$ th fiber section is  $E_{T_\sigma}$ . The total energy loss on the  $\sigma$ th fiber section just after the mode filter is, thus,

$$E_{T_{\sigma+1}} - E_{T_\sigma} = - \left[ \frac{N_N}{N_{T_p} + N_N} e^{-2\alpha d} + (1 - e^{-2\alpha d}) \right] E_{T_\sigma}. \quad (70)$$

The symbol  $\alpha$  indicates the losses caused by absorption and random scattering. We solve the difference equation and use the relation

$$\sigma d = z \quad (71)$$

to obtain with the help of (68) (with  $M = N$ ) and (69),

$$E_{T_\sigma} = E_{T_0} \left( \frac{N+1}{N+3} \right)^\sigma e^{-2\alpha z}. \quad (72)$$

At the end of the fiber, we have a total of  $L/d$  mode filter sections. The excess loss caused by the mode filters is, thus,

$$\frac{E_{TL}}{E_{T_0}} e^{2\alpha L} = \left( \frac{N+1}{N+3} \right)^{L/d} = e^{-2\alpha_f L}. \quad (73)$$

This allows us to define the approximate power-loss coefficient per unit length for the excess filter-loss penalty,

$$2\alpha_f = \frac{2}{Nd} = \frac{3.5}{n_0 k a \sqrt{2\Delta} d}. \quad (74)$$

Equation (52) was used to obtain the right-hand side of this expression. Short fiber sections of length  $d$  between mode filters (in other words, more mode filters) thus increase the excess loss.

## VI. DISCUSSION AND NUMERICAL EXAMPLES

In the introduction, we have outlined our strategy for reducing pulse spreading in parabolic-index fibers. We are now in a position to offer specific design criteria for our approach. The most important aspect of the fiber design consists in incorporating index fluctuations into the fiber core that obey the relation (30). As pointed out earlier, the  $r$  dependence of the index perturbations is not particularly important.

The linear dependence was chosen for convenience. The function  $f(z)$  is a nearly periodic, random function that must contain spatial frequencies in the range

$$\left. \begin{aligned} \theta &= \frac{2\pi}{\Lambda} = \frac{\sqrt{2\Delta}}{a} \rightarrow \frac{\sqrt{2\Delta}}{a} + \delta\theta \\ \text{with } \delta\theta &= 1.15 \theta\Delta \end{aligned} \right\}. \quad (75)$$

[This formula follows from (2) and (26) with the help of (16), (18), (22), with  $\delta M = 1$ , and (52)]. The parameter  $\Delta$  is defined by (3). For the numerical example given by (21), we find that  $\theta a$  ( $a$  is the fiber-core radius) covers the range from 0.14 to 0.1415. To gain insight into the meaning of these numbers, we assume that the vacuum wavelength of the light transmitted through our fiber is  $\lambda = 1 \mu\text{m}$ . This means that  $ka = 150$  leads to a core radius of  $23.87 \mu\text{m}$ . The spatial period length of the almost periodic random function must thus be  $\Lambda = 1.07 \text{ mm}$ .

Next, we must decide what amount of index fluctuation is required to achieve a desired reduction in the width of the uncoupled pulse (pulse carried by uncoupled modes). In the absence of coupling, the pulse width is given by

$$T_{uc} = \frac{n_0 L}{2c} \Delta^2. \quad (76)$$

The pulse width in the presence of mode coupling must be smaller than this value, otherwise steady state has not been reached and (50) and (51) are not applicable. First, let us consider how much harm results from coupling between P-modes and the unwanted group of S-modes along the common mode boundary. Using the values in (21), we find from (52) that  $N = 18$ . Let us (arbitrarily) assume that  $\rho = 1$ ; we then find from (50) that the pulse width of the coupled modes is 28 percent larger than the width of coupled P-modes in the absence of S-mode coupling. Ignoring the slight pulse-broadening effect of residual S-mode coupling, we define an improvement factor  $R$  as

$$R = \frac{T_0}{T_{uc}}. \quad (77)$$

It is desirable to make  $R$  as small as possible and only values with  $R < 1$  are meaningful. From (51), (52), and (76) we get

$$R = \frac{1.41 n_0^2 \Delta^{\frac{1}{2}}}{\left(\frac{L}{a^2} \langle F^2(\theta) \rangle\right)^{\frac{1}{2}}} = \frac{0.33}{\left(\frac{L}{a^2} \langle F^2(\theta) \rangle\right)^{\frac{1}{2}}}. \quad (78)$$

The numerical value on the right-hand side was obtained with the

help of (21). To achieve, for example,  $R = 0.1$  would require

$$\left[ \frac{L}{a^2} \langle F^2(\theta) \rangle \right]^{\frac{1}{2}} = 3.3.$$

To understand what this result means in terms of the amplitude of the refractive-index fluctuations, let us consider that the function  $f(z)$  appearing in (30) has the form

$$f(z) = A \sin [\Omega z + \psi(z)], \quad (79)$$

where  $\psi(z)$  is a random phase function with correlation length  $D_{\text{corr}}$ . The power spectrum of this function defined by (1) is<sup>4</sup>

$$\langle F^2(\theta) \rangle = A^2 \frac{\sin^2 \left[ (\theta - \Omega) \frac{D_{\text{corr}}}{2} \right]}{(\theta - \Omega)^2 D_{\text{corr}}}. \quad (80)$$

Instead of the correlation length  $D_{\text{corr}}$ , we may introduce the width  $\delta\theta$  of the spectral band by the relation

$$\delta\theta = \frac{4\pi}{D_{\text{corr}}}. \quad (81)$$

With  $\Omega = \theta$ , we thus obtain from (80) and (81)

$$\left[ \frac{L}{a^2} \langle F^2(\theta) \rangle \right]^{\frac{1}{2}} = A \left( \frac{\pi}{a\delta\theta} \frac{L}{a} \right)^{\frac{1}{2}} = 3.3. \quad (82)$$

(The number on the right-hand side pertains to our example.) This important relation shows how the amplitude  $A$  of the refractive-index fluctuations is related to the spectral bandwidth  $\delta\theta$ , the core radius, and the length of fiber over which a certain improvement factor  $R$  (in our case  $R = 0.1$ ) is to be achieved. For our example,  $\theta a$  ranges from 0.14 to 0.1415 so that we have  $a\delta\theta = 0.0015$ . Assuming  $L = 1$  km, and using  $a = 23.87 \mu\text{m}$ , we have from (82)

$$A = 1.1 \times 10^{-5}. \quad (83)$$

The refractive-index fluctuations follow from (30) and (79) if we assume that  $\mathbf{n} - n \ll 1$  [ $n$  is the perfect index distribution (5)]:

$$\mathbf{n} - n = \frac{1}{2n_0} \frac{r}{a} A \sin [\theta z + \psi(z)] \cos \phi. \quad (84)$$

It is apparent from (83) that very slight index fluctuations are very effective for intentional mode coupling. Much more substantial pulse-length shortening than  $R = 0.1$  should, thus, be easily achievable. The random phase fluctuations with correlation length  $D_{\text{corr}}$  can be produced by keeping the phase  $\psi(z)$  of (79) constant over a fixed

distance and introducing a random phase jump periodically in length intervals  $D_{\text{corr}}$ . The relation between  $D_{\text{corr}}$  and the desired bandwidth of the random function is given by (81) and (75).

Not much has been said about the problem of actually implementing the refractive-index fluctuations prescribed by (30) or (84). In principle, it is possible to introduce the refractive-index fluctuation during the process of preform fabrication, since it is necessary to take special care to produce the parabolic-index profile in any case. It may thus be possible to produce the intentional deviations from the perfect parabolic-index profile in the core by programming the process of chemical vapor deposition, or whatever process is used to control the refractive-index profile. However, there is a much simpler way of realizing a refractive-index fluctuation of the kind required by (30). Let us write the index profile inside the fiber core in cartesian coordinates:

$$n = n_0 \left[ 1 - \frac{x^2 + y^2}{a^2} \Delta \right]. \quad (85)$$

If we displace the index profile in  $x$  direction from its symmetric position, we may make the substitution

$$x \rightarrow x - g.$$

Assuming the displacement  $g$  to be small, we obtain instead of (85)

$$\mathbf{n} = n + 2n_0 \frac{xg}{a^2} \Delta \quad (86)$$

with  $n$  once more given by (85). By transforming the cartesian coordinates to cylindrical coordinates using

$$x = r \cos \phi, \quad (87)$$

we obtain

$$\mathbf{n}^2 - n^2 \approx 2n_0(\mathbf{n} - n) = \frac{r}{a} \left( 4n_0^2 g \frac{\Delta}{a} \right) \cos \phi. \quad (88)$$

Comparison of (30) and (88) allows us to make the following association:

$$f(z) = 4n_0^2 g \frac{\Delta}{a}. \quad (89)$$

The actual displacement of the fiber axis from perfect straightness can be expressed as

$$g = B \sin [\Omega z + \psi(z)], \quad (90)$$

with  $B$  being the displacement amplitude. Comparison of (79), (89),

and (90) allows us to use the relation

$$B = \frac{aA}{4n_0^2\Delta}. \quad (91)$$

For our example values (21), we thus obtain from (83)

$$B = 2.9 \times 10^{-3} \mu\text{m}. \quad (92)$$

This discussion shows that we may introduce the desired perturbation by actually bending the fiber axis in the form indicated by (90) with the very small amplitude  $B$ . Such bending could be accomplished by surrounding the fiber with a suitably strained plastic jacket.

The abrupt refractive-index discontinuity of magnitude  $n_0(1 - \Delta) - n_2$  is necessary to insulate the P-modes from the radiation modes by creating a buffer region of S-modes. The amount of this index step is actually quite arbitrary. However, it is clear from the general formula (65) for the signal-to-noise ratio that the sum over  $n$  in the denominator of this expression is larger when it consists of more terms, that is, if there are more S-modes. To keep the signal-to-noise ratio as small as possible requires keeping the number of S-modes small, which is achieved by keeping the abrupt index discontinuity small. What is the minimum index step that is needed for effective isolation of the P-modes? We can estimate a minimum index step by the following consideration. The lowest possible value of the propagation constant of P-modes is given by

$$\beta_m = n_0(1 - \Delta)k. \quad (93)$$

The largest propagation constant of the radiation modes (actually, what we call radiation modes become cladding modes in a fiber with finite cladding thickness) is given by

$$\beta_r = n_2k. \quad (94)$$

Adjacent groups of P-modes with the same value  $M$  of the compound mode number are spaced a distance  $\theta$  (in  $\beta$ -space) apart. A sufficiently wide buffer zone of S-modes is required to isolate the P-modes from radiation modes. Thus, we require that the P-mode group with propagation constant (93) is separated (in  $\beta$ -space) by  $3\theta$  from the radiation modes. This requirement leads us to the desired condition for the minimum height of the index step

$$n_0(1 - \Delta) - n_2 = \frac{3\theta}{k} = 3 \frac{\sqrt{2\Delta}}{ka}. \quad (95)$$

For the values listed in (21), we find  $n_0(1 - \Delta) - n_2 = 0.003$ .

It remains to consider the design of the mode filters. Mode filters consist of fiber sections with the refractive index distribution of Fig.



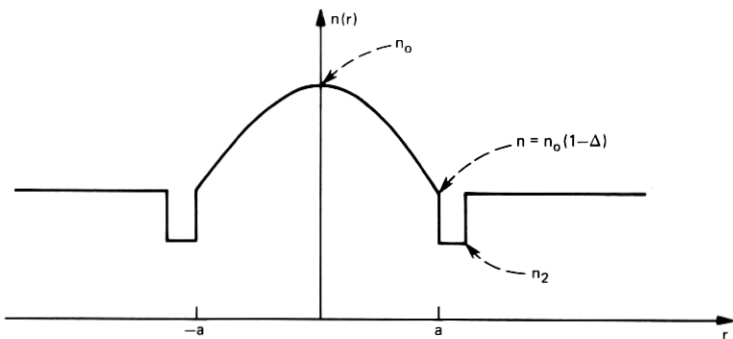


Fig. 5—Refractive-index profile of a fiber providing continuous mode filtering for S-modes by electromagnetic tunneling.

1b and serve the purpose of stripping off S-modes. The length of the filter sections depends on the S-mode losses of the filters. Since S-modes are leaky waves on the filter sections, their losses are very high, so that filters 10 cm to 1 m long should be sufficient. We have seen that the signal-to-noise ratio (66) increases as the distance  $d$  between mode filters decreases. The only limitation on the length of  $d$  or the number of mode filters  $L/d$  is the additional loss caused by the filters. If we decide to tolerate an additional filter loss of 1 dB/km ( $2\alpha_f = 0.23 \text{ km}^{-1}$ ) for the entire fiber, we find from (74) with the numbers of (21)

$$d = 0.47 \text{ km.} \quad (96)$$

If the filter spacing is reduced below this distance, the filter-loss contributions increase above 1 dB/km.

The signal-to-noise ratio that is caused by unintentional coupling between P-modes and S-modes can be computed from (66) if a calibration measurement has been made. In principle, it would be possible to compute this value from (65); however, such a calculation would require a detailed knowledge of the unintentional power-coupling coefficients  $H_{\nu n}$ . In the absence of accurate information of unintentional fiber imperfections, such a calculation is not possible.

Instead of using discrete mode filters spaced at certain intervals it is also possible to design the fiber so that mode filtering is achieved continuously over its entire length. The index profile of such a fiber is shown in Fig. 5.

## VII. ACKNOWLEDGMENT

E. A. J. Marcatili suggested the possibility of implementing the intentional fiber perturbations by bending the fiber axis and of using a fiber designed with continuous mode filters. Illuminating discussions with him are also gratefully acknowledged.

## REFERENCES

1. D. Gloge and E. A. J. Marcatili, "Multimode Theory of Graded-Core Fibers," *B.S.T.J.*, *52*, No. 9 (November 1973), pp. 1563-1578.
2. D. Marcuse, *Theory of Dielectric Optical Waveguides*, New York: Academic Press, 1974.
3. D. Personick, "Time Dispersion in Dielectric Waveguides," *B.S.T.J.*, *50*, No. 3 (March 1971), pp. 843-859.
4. D. Marcuse, "Reduction of Pulse Dispersion by Intentional Mode Coupling," *B.S.T.J.*, *53*, No. 9 (November 1974), pp. 1795-1815.
5. D. Marcuse, "Coupled Mode Theory of Round Optical Fibers," *B.S.T.J.*, *53*, No. 6 (July-August 1973), pp. 817-842.
6. D. Gloge, "Propagation Effects in Optical Fibers," *IEEE Trans. Microw. Theory Tech.*, *MTT-23*, No. 1 (January 1975), pp. 106-120.
7. D. Gloge, "Weakly Guiding Fibers," *Appl. Opt.*, *10*, No. 10 (October 1971), pp. 2252-2258.
8. K. Petermann, "The Mode Attenuation in General Graded Core Multimode Fibers," *Arch. Elec. Uebertr.* *29*, No. 7/8 (July-August 1975), pp. 345-348.
9. G. Goubau and F. Schwering, "On the Guided Propagation of Electromagnetic Beam Waves," *IRE Trans. Ant. Propag.*, *AP-9*, No. 3 (May 1961), pp. 248-256.
10. H. Kogelnik and T. Li, "Laser Beams and Resonators," *Appl. Opt.*, *5*, No. 10 (October 1966), pp. 1550-1567.
11. D. Marcuse, "Excitation of Parabolic-Index Fibers With Incoherent Sources," *B.S.T.J.*, *54*, No. 9 (November 1975), pp. 1507-1530.
12. D. Marcuse and H. M. Presby, "Mode Coupling in an Optical Fiber with Core Distortions," *B.S.T.J.*, *54*, No. 1 (January 1975), pp. 3-15.
13. L. S. Watkins, "Instrument for Continuously Monitoring Fiber Core and Outer Diameters," *Optical Fiber Transmission*, A digest of technical papers presented at the Topical Meeting on Optical Fiber Transmission, January 7-9, 1975, Williamsburg, Virginia; Washington, D. C.: Optical Society of America, 1975, pp. TuA4-1 to TuA4-4.
14. D. Gloge, "Optical Power Flow in Multimode Fibers," *B.S.T.J.*, *51*, No. 8 (October 1972), pp. 1767-1783.